Environmental and Experimental Botany 144 (2017) 76–87

Contents lists available at ScienceDirect

Environmental and Experimental Botany

journal homepage: www.elsevier.com/locate/envexpbot

A glimpse into the physiological, biochemical and nutritional status of soybean plants under Ni-stress conditions

André Rodrigues dos Reis[a,b,*], Jéssica Pigatto de Queiroz Barcelos[b], Christian Rones Wruck de Souza Osório[c], Elcio Ferreira Santos[d], Lucas Aparecido Manzani Lisboa[e], José Mateus Kondo Santini[b], Maria José Dornelas dos Santos[a], Enes Furlani Junior[b], Marcelo Campos[b], Paulo Alexandre Monteiro de Figueiredo[e], José Lavres[d], Priscila Lupino Gratão[f]

[a] São Paulo State University - UNESP, 17602-496, Tupã, SP, Brazil
[b] São Paulo State University - UNESP, 15385-000, Ilha Solteira, SP, Brazil
[c] Federal University of Mato Grosso do Sul - UFMS, 79540-000, Chapadão do Sul, MS, Brazil
[d] University of São Paulo - USP, 13416-000, Piracicaba, SP, Brazil
[e] São Paulo State University - UNESP, 17900-000, Dracena, SP, Brazil
[f] São Paulo State University – UNESP, 79560-000, Jaboticabal, SP, Brazil

ARTICLE INFO

Keywords:
Ni phytotoxicity
Oxidative stress
Gas exchange
Ni toxicity
Glycine max L

ABSTRACT

Nickel (Ni) toxicity has been reported to decrease productivity in soybean (*Glycine max* L.). However, soybean responses to Ni toxicity are not well understood. The aim of the present study was to describe Ni toxicity in soybean plants through physiological, nutritional, and ultrastructural analyses. Plants were grown in nutrient solution containing increasing Ni concentrations (0, 0.05, 0.1, 0.5, 10, and 20 μmol L^{-1}), and nutritional, anatomical, physiological and biochemical features were determined. The results revealed previously unreported detrimental effects of Ni toxicity on soybean plants. CO_2 assimilation rates, stomatal conductance and transpiration decreased, resulting in lower biomass in soybean plants exposed to the highest Ni levels. Nitrate reductase activity increased with up to 0.05 μmol L^{-1} Ni and then decreased, indicating halted N-metabolism. Urease activity increased with increasing Ni availability in the nutrient solution, and peroxidase and superoxide dismutase activities were higher in plants grown at higher Ni levels. Leaf epidermal thickness (abaxial and adaxial), as well as root xylem and phloem diameter, decreased starting at 0.1 μmol L^{-1} Ni. Mean Ni concentrations varied from 77.5 to 17,797.4 mg kg^{-1} in roots and 2.3 to 16,774.5 mg kg^{-1} in shoots. Soybean plants exhibited symptoms of Ni toxicity starting at 0.1 μmol L^{-1} Ni, presenting mean shoot Ni concentration of 28.9 mg kg^{-1}, along with leaf water loss until complete drying. The results contribute to our understanding of several physiological, biochemical and histological mechanisms of Ni toxicity in soybean, which is still poorly understood.

1. Introduction

Decreases in crop productivity are frequently caused by biotic and abiotic stresses (Reis et al., 2015). Heavy metal stress is an abiotic stress with important effects on agricultural systems, especially due to the global increase in soil and water pollution (Ahmad et al., 2015). Some metals are required by plants in small amounts, with the thresholds of essentiality and toxicity being very close (Santos et al., 2017). Nickel (Ni) is an essential metal for plants because it is a structural component of the metalloenzyme urease (EC 3.5.1.5., urea amidohydrolase), which is responsible for the conversion of urea into carbon dioxide (CO_2) and ammonia (NH_3) (Dixon et al., 1975), playing an important role in nitrogen metabolism (Polacco et al., 2013; Lavres et al., 2016; Macedo et al., 2016). Ni also activates an isoform of glyoxalase I, which participates in the degradation of cytotoxic compounds (Fabiano et al., 2015). However, high Ni concentrations cause plant toxicity.

Abbreviations: *A*, CO_2 assimilation rate; C_i, capacity of internal carbon use; ABET, epidermal thickness of the lower or abaxial face; ADET, epidermal thickness of the upper or adaxial face; CAT, catalase; *E*, transpiration; *Gs*, stomatal conductance; LPD, leaf phloem diameter; LXD, leaf xylem diameter; PAR, photosynthetically active radiation; POD, peroxidase; RET, root epidermis thickness; ROS, reactive oxygen species; RPD, root phloem diameter; RXD, root xylem diameter; SOD, superoxide dismutase

* Corresponding author at: São Paulo State University - UNESP, Rua Domingos da Costa Lopes, 780 SP, Tupa 17602-496, Brazil.
E-mail addresses: andrereis@tupa.unesp.br, andrekun@gmail.com (A.R.d. Reis).

http://dx.doi.org/10.1016/j.envexpbot.2017.10.006
Received 23 June 2017; Received in revised form 30 September 2017; Accepted 5 October 2017
Available online 05 October 2017
0098-8472/

Ni concentrations in the earth's crust are relatively low (approximately 20 mg kg^{-1}), except for soils of ultramafic origin, in which Ni concentrations may vary between 1400 and 2000 mg kg^{-1} (Kabata-Pendias and Pendias, 2011) and reach 7100 mg kg^{-1} in serpentine soils (Uren, 1992). However, soil Ni concentrations may increase due to contamination by metal-processing plants, oil and carbon combustion, and the use of sewage sludge and phosphate fertilizers in agriculture (Kabata-Pendias and Pendias, 2011).

Only two plant species have been reported to exhibit Ni-deficiency symptoms under field conditions: *Carya illinoinensis* (Wood et al., 2006) and *Betula nigra* (Ruter, 2005). Ni is therefore often reported to be a toxic element. The observed cases of highest Ni toxicity were mainly due to low Ni requirement by crops (0.05 and 10 mg kg^{-1} dry mass) (Küpper and Kroneck, 2007; Küpper and Andresen, 2016). Furthermore, the difference between adequate and toxic Ni concentrations is extremely small compared with other heavy metals, whose concentrations in plants are higher than 10 mg kg^{-1} dry mass (Kabata-Pendias and Pendias, 2011).

In polluted soils, the total Ni concentration ranged from 200 to 26,000 mg kg^{-1} (Sreekanth et al., 2013). However, there are very few reports in the literature on the Ni free in contaminated soil pore waters. Nolan et al. (2009) related that the pore water free Ni^{+2} ranged from 5 to 250 µmol. Thus, the Ni accumulation and bioavailability to plants has gained great attentions recently, due to their potential health risks and food safety problems (Kabata-Pendias and Pendias, 2011).

Visual symptoms of Ni toxicity include chlorosis followed by necrosis (Gajewska et al., 2006; Seregin and Kozhevnikova, 2006; Ahmad et al., 2007), with yellowing between veins, similar to what is observed in manganese (Mn) deficiency (Hewitt, 1953). Ni toxicity also affects root and shoot growth. In more severe cases, it causes deformity of several plant parts and brown spots in leaves (Mishra and Kar, 1974). In addition, excess Ni leads to decreased mesophyll thickness by decreasing the intercellular spaces of the palisade and spongy parenchyma (Molas, 1997) and affects the size and diameter of main and lateral vessels, as well as the width of leaf epidermal cells (Seregin and Kozhevnikova, 2006).

Excess soil Ni causes an imbalance in ion uptake due to competitive inhibition, decreasing the uptake of iron (Fe), zinc (Zn), copper (Cu) and Mn, among others (Seregin and Ivanov, 2001; White, 2012; Nishida et al., 2015; Küpper and Andresen, 2016), and affecting aspects of plant metabolism that are dependent on these metals, e.g., the enzymes catalase and peroxidase (Granick, 1951; Kazemi et al., 2010; Sirhindi et al., 2016). In addition, Ni toxicity affects photosynthesis by inhibiting the electron transport chain and degrading photosystems I and II (Tripathy et al., 1983; Mohanty et al., 1989; Seregin and Ivanov, 2001). Ni toxicity may also disrupt chloroplast structure, block chlorophyll synthesis (Polacco et al., 2013), and inactivate Calvin cycle enzymes (Sheoran et al., 1990; Seregin and Ivanov, 2001).

Ni excess in plants leads to stomatal closure, limiting CO_2 uptake (Sheoran et al., 1990; Bishnoi et al., 1993), and increased formation of reactive oxygen species, which damage several biomolecules (Ahmad, 2013; Ahmad et al., 2015; Sirhindi et al., 2016). Plants tend to decrease Ni stress by increasing the activity of antioxidant enzymes, such as superoxide dismutase, catalase, and peroxidase (Schickler and Caspi, 1999; Pandolfini et al., 1992; Seregin and Ivanov, 2001; Kazemi et al., 2010; Sirhindi et al., 2016). Although physiological disorders caused by Ni toxicity have been reported for different plant species, the physiological responses of soybean plants exposed to excess Ni are not well described. The hypothesis of this work is that soybean plants under Ni stress has the nutritional, anatomical and physiological characteristics impaired, reducing its growth and development. Thus, the aim of the present study was to describe Ni toxicity in soybean plants through physiological, nutritional and ultrastructural analyses.

2. Materials and methods

2.1. Growth conditions and experimental design

Soybean seeds of the variety BMX Potência RR were germinated in plastic pots with vermiculite. Uniform young seedlings at 21 days after sowing were washed with deionized water and transplanted into 6-L polyethylene pots containing nutrient solution with 25% ionic strength and lacking Ni (Hoagland and Arnon, 1950). After 5 days of plant adaptation to these nutrient solutions, Ni treatments of 0 (control), 0.05, 0.1, 0.5, 10, and 20 µmol L^{-1}, with 100% ionic strength in the nutrient solution, were applied. Constant aeration was maintained in all pots.

The experimental design was completely randomized, with four replicates. Ni was provided in the form of $NiCl_2$. The complete nutrient solution contained 12.0 mmol L^{-1} $N\text{-}NO_3^-$, 4.0 mmol L^{-1}0 $N\text{-}NH_4^+$, 2.0 mmol L^{-1} phosphorus (P), 6.0 mmol L^{-1} of potassium (K), 4.0 mmol L^{-1} calcium (Ca), 2.0 mmol L^{-1} magnesium (Mg), 2.0 mmol L^{-1} sulfur (S), 25.0 µmol L^{-1} boron (B), 0.5 µmol L^{-1} Cu, 54.0 µmol L^{-1} Fe, 2.0 µmol L^{-1} Mn, 2.0 µmol L^{-1} Zn, and 0.5 µmol L^{-1} molybdenum (Mo). The initial pH (approximately 5.0 ± 0.5) was monitored daily in each experimental unit to ensure the availability of Ni; this pH range was fixed throughout the experiment. Estimates of the Ni species were obtained using Visual Minteq version 3.1 software (Gustafsson, 2011), and in all of treatments, approximately 90% of the Ni was available (Ni^{2+}) for ready uptake.

Gas exchange, urease activity, and nitrate reductase activity tests, as well as extraction of antioxidant enzymes and proteins, were performed 48 h after plant exposure to Ni between 8:00 and 12:00 AM, using the first fully developed trifoliate. Antioxidant enzymes and proteins were also extracted from roots. At the end of the experiment, when the symptoms of Ni toxicity had worsened (7 days of exposure to Ni), the first fully developed trifoliate was collected for leaf diagnosis (Lavres Junior et al., 2009, 2010) and to characterize the symptoms of Ni toxicity (leaf morphology and scanning electron microscopy).

2.2. Gas exchange parameters

Gas exchange was evaluated via non-destructive analyses using a portable gas exchange device (Infra-Red Gas Analyzer −IRGA, brand ADC BioScientific Ltd, model LC-Pro). The following parameters were determined: CO_2 assimilation rate expressed by area (A − µmol CO_2 m^{-2} s^{-1}), transpiration (E − mmol H_2O m^{-2} s^{-1}), stomatal conductance (G_S − mol H_2O m^{-2} s^{-1}), and internal CO_2 concentration in the substomatal chamber (C_I − µmol mol^{-1}). The initial conditions imposed for the measurements were 1000 µmol m^{-2} s^{-1} of photosynthetically active radiation (PAR), provided by LED lamps, 380 ppm of CO_2, and a chamber temperature of 28 °C, according to Santos et al. (2017).

2.3. Activity of urease (EC 3.5.1.5)

Urease activity was measured according to the whole-tissue method of Hogan et al. (1983) and with ammonium determination as suggested by McCullough (1967). One hundred milligrams of fresh tissue cut in discs was transferred to assay tubes containing 8 mL of 50 mM phosphate buffer (pH 7.4), 0.2 M urea, and 0.6 M *n*-propanol for a period of 3 h. After incubation, a 0.5-mL aliquot of supernatant was added to 2.5 mL of Reagent I (0.1 M phenol and 170 µM sodium nitroprusside). Afterward, 2.5 mL of Reagent II (0.125 M NaOH + 0.15 M $Na_2HPO_4{\cdot}12H_2O$ + NaOCl (3% Cl_2)) was added for the determination of ammonium. This reaction was performed in capped assay tubes under continuous shaking in a water bath at 37 °C for 35 min. Ammonium was measured in a spectrophotometer at 625 nm using a NH_4Cl standard calibration curve, and urease activity was expressed as µmol $N\text{-}NH_4^+$ h^{-1} g^{-1} FW (fresh weight).

2.4. Activity of nitrate reductase (EC 1.7.1.1)

In vivo nitrate reductase activity was determined according to Reis et al. (2009) with slight modifications. Leaf samples were collected at 8:30 AM, stored in plastic bags, and transported to the laboratory on ice. Afterward, 200 mg of fresh tissue cut in discs was transferred to assay tubes containing 5 mL of phosphate buffer solution, pH 7.5 (100 mM potassium phosphate buffer + 100 mM KNO_3). Thereafter, the assay tubes (wrapped in aluminum foil to protect them from light) were incubated in a 30 °C water bath for 60 min. The reaction was performed with 100 µL of supernatant + 1.9 mL of distilled water + 0.5 mL of 1% sulfanilamide in 2 M HCl, followed by 0.5 mL of 0.02% naphtylenediamine solution. The nitrite (NO_2^-) produced was measured in a spectrophotometer at 540 nm using a nitrite standard calibration curve. Enzyme activity was directly related to the amount of NO_2^-, and the results were expressed in µmol NO_2^- g^{-1} h^{-1} FW.

2.5. Extraction of antioxidant enzymes and proteins

Plant material was macerated in a mortar containing liquid nitrogen. Protein extracts were obtained from 1.5 g of fresh plant material, together with the addition of PVPP (polyvinylpolypyrrolidone) corresponding to 20% (w:v). Protein extraction proceeded using a potassium phosphate buffer solution at 100 mmol L^{-1} (pH 7.5), EDTA (ethylenediaminetetraacetic acid) at 1 mmol L^{-1}, and DDT (dithiothreitol) at 1 mmol L^{-1}. The homogenized extracts were centrifuged at 10,000 rpm for 30 min at 4 °C. The supernatant was collected in Eppendorf tubes, frozen in liquid nitrogen, and stored at −80 °C. The soluble protein concentration was determined by the method of Bradford (1976) using BSA (bovine serum albumin) as a standard. Aliquots of 100 µL of extract were mixed with 5 mL of Bradford reagent with four replicates. Readings were performed on a spectrophotometer at 595 nm. The results were used to calculate the antioxidant enzyme concentrations.

2.6. Peroxidase activity (POD, EC. 1.11.1.7)

The method of Allain et al. (1974) was used to determine the POD activity present in the leaf tissues of soybean. From tissue extracts obtained by the enzymatic extraction process described above, 0.5-mL aliquots were removed and added to 0.5 mL of 0.2 M potassium phosphate buffer (pH 6.7), 0.5 mL of H_2O_2 (hydrogen peroxide), and 0.5 mL of aminoantipyrine. The tubes were placed in a water bath at 30 °C for 5 min. After incubation, 2 mL of ethanol was added to stop the reaction, and after being cooled to room temperature, the samples were vortexed and read on a spectrophotometer (λ = 505 nm). As a control, the enzyme extract was replaced with 0.2 M potassium phosphate buffer (pH 6.7). The total enzyme activity was expressed in µmol de H_2O_2 min^{-1} mg^{-1} of protein.

2.7. Superoxide dismutase activity (SOD, EC 1.15.1.1)

SOD activity was determined according to Giannopolitis and Ries (1977). The reaction was conducted in a reaction chamber (box) under illumination with a 15 W fluorescent lightbulb at 25 °C. An aliquot (50 µL) of the sample was added to a 5-mL mixture of sodium phosphate buffer (50 mmol L^{-1}), pH 7.8, methionine (13 mmol L^{-1}), NBT (75 mmol L^{-1}), EDTA (0.1 mmol L^{-1}), and riboflavin (2 µmol L^{-1}). The tubes were placed inside the box, closed to any external light, and maintained under box lighting for 15 min for the formation of the blue formazan compound produced by the photoreaction of NBT. Other tubes containing the same mixture were covered with aluminum foil to prevent light exposure; these test tubes served as the control for each sample. After 15 min, the material was homogenized by vortexing. Readings were taken on a spectrophotometer at 560 nm, and the results were expressed as U SOD mg^{-1} protein.

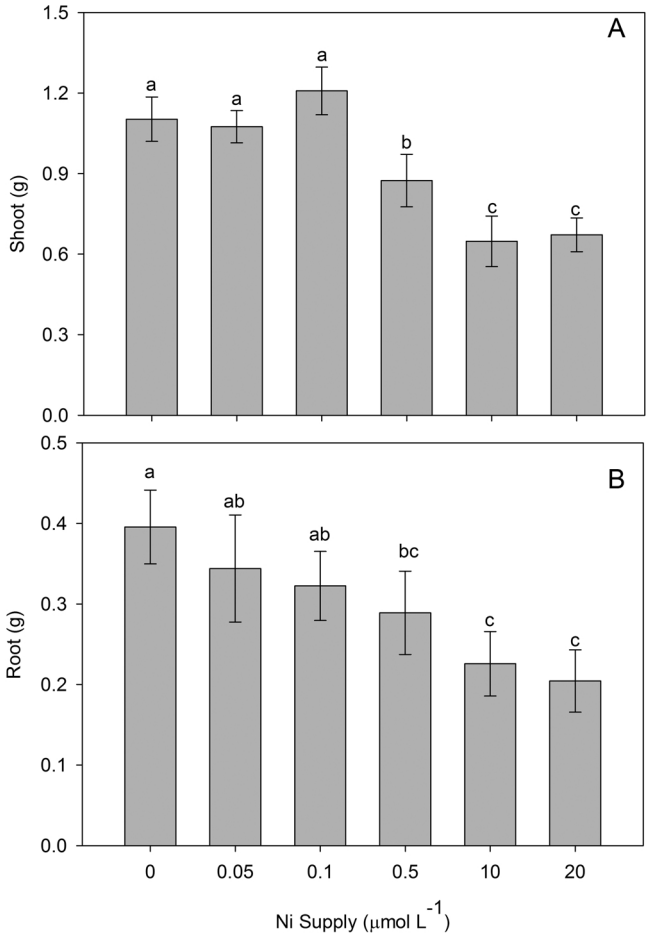

Fig. 1. Dry mass of shoots (A) and roots (B) of soybean plants grown at different Ni concentrations in the nutrient solution. Letters indicate significant differences at P ≤ 0.05. Error bars indicate the standard error (n = 4).

2.8. Catalase activity (CAT, EC 1.11.1.6)

CAT activity was determined by monitoring the degradation of H_2O_2 at 240 nm according to the method of Azevedo et al. (1998). First, 1 mL of 100 mM potassium phosphate buffer, pH 7.5, and 2 µL of H_2O_2 30% were added to each tube, followed by 150 µL of protein extract. Immediately after the addition of the protein extract, the tubes were quickly mixed by vortexing. Enzyme activity was determined by the decomposition of H_2O_2 during a 2-min interval in a spectrophotometer at a wavelength of 240 nm at 25 °C. The results were expressed in µM min^{-1} mg^{-1} protein.

2.9. Dry mass production of the plants

At harvest (phonological stage V4), the plants were separated into shoots (leaves + stem) and roots. The material was identified, packaged in paper bags, and dried in an oven at ± 65 °C for 2 days, followed by the measurement of dry mass.

2.10. Chemical analysis of plant tissue

The concentrations of P, K, Ca, Mg, S, B, Cu, Fe, Mn, and Zn were determined in the shoots and roots. Nitric-perchloric digestion was performed (Miller, 1998), and the identity and amount of nutrients were determined using radial visualization on an inductively coupled plasma optical emission spectrometer (ICP-OES) equipped with a nebulization chamber. The following emission lines were used: P $_I$ 213.618 nm; K $_I$ 769.897 nm; Ca $_I$ 422.673 nm; Mg $_I$ 280.270 nm; S $_I$

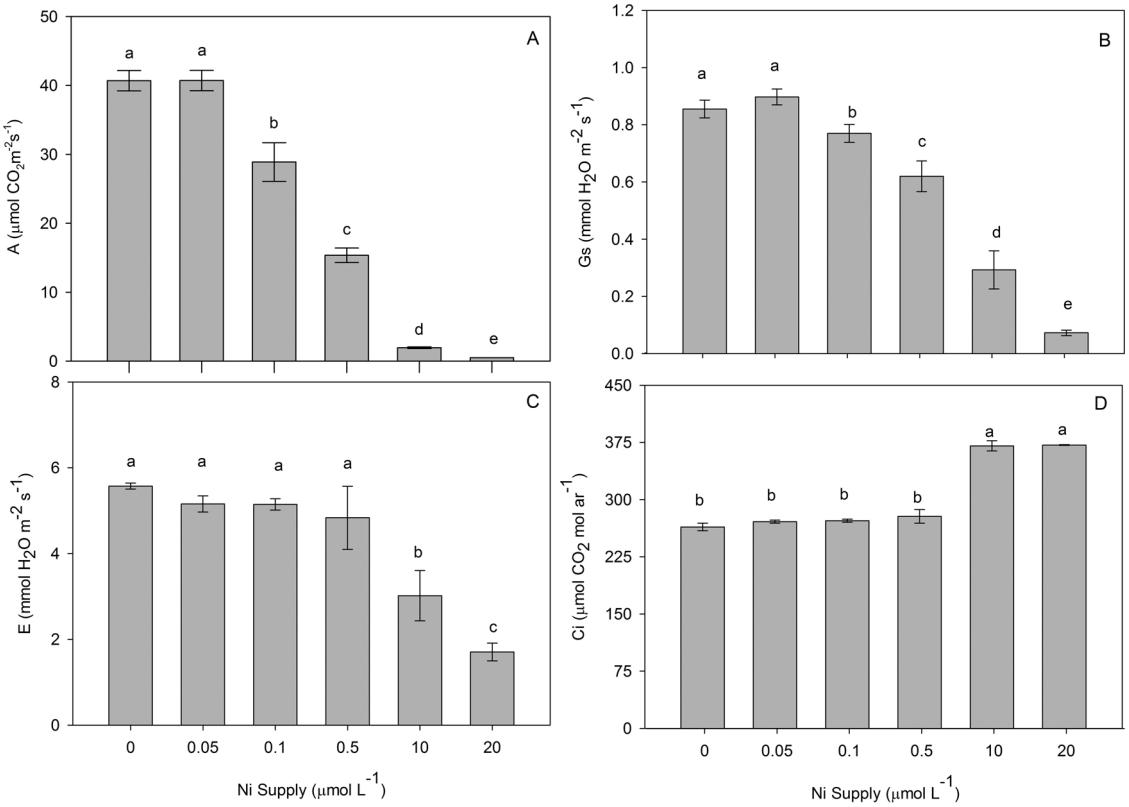

Fig. 2. (A) Net photosynthetic rate (A), (B) internal CO_2 concentration (C_i), (C) transpiration rate (E), and (D) stomatal conductance (Gs) in soybean plants grown at different Ni concentrations in the nutrient solution. Letters indicate significant differences at $P \leq 0.05$. Error bars indicate the standard error (n = 4).

181.972 nm; B $_{I}$ 249.773 nm; Cu $_{I}$ 324.754 nm; Fe $_{II}$ 259.940 nm; Mn $_{II}$ 259.373 nm; Zn $_{II}$ 231.865 nm; and Ni $_{II}$ 231.604.

2.11. Leaf and root morphology

After 7 days of exposure to Ni (phonological stage V1), plants were collected for symptomatology and histological analysis. Leaf and root fragments were collected and fixed in F.A.A. 70 solution (37% formaldehyde and acetic acid and 70% ethanol at a ratio of 1.0:1.0:18.0–V/V) and stored until analysis according to the method described by Santos et al. (2017).

All plant tissue fragments received the relevant procedures for dehydration, diafanization, inclusion, and fixation. With the aid of a Leica microtome table containing a steel blade, 8- to 14-μm sections were cut from each embedded fragment. For the histological slides, the first cross-sections that showed the best preserved material were selected, i.e., without damage or injury caused by cutting the plant tissue. All of the chosen sections were fixed with Mayer adhesive, stained with 1% safranin, and mounted on slides and cover slips with Entellan adhesive. All of the slides were observed on an Olympus optical microscope with a coupled camera to measure anatomical parameters using the CellSens Standard image analysis program, calibrated with a microscopic rule at the same zoom level of the photographs.

In the midrib region of the leaves in the cross-sections, the following morphoanatomic characteristics were observed: epidermal thickness of the lower or abaxial face (ABET), epidermal thickness of the upper or adaxial face (ADET), leaf phloem diameter (LPD), and leaf xylem diameter (LXD). The morphoanatomic root characteristics obtained were root epidermis thickness (RET), root phloem diameter (RPD), and root xylem diameter (RXD) (Carlquist, 1975). For each characteristic, 10 measurements were performed per slide. Plots show the mean values obtained for each characteristic.

2.12. Scanning electron microscopy

Leaf and root plant material was fixed in modified Karnovsky fixative (2.5% glutaraldehyde and 2.5% formaldehyde in 0.05 M sodium cacodylate buffer, pH 7.2), post-fixed with osmium tetroxide (OsO_4), and dehydrated in increasing solutions of acetone (30, 50, 70, 90, and 100%). Subsequently, the specimens were dried to their critical point with liquid CO_2 (Balzers CPD 030), sputter-coated (MED 010 Balzers) with a thin layer of gold, and examined on a scanning electron microscope (EVO-LS15-ZEIS), as described in our previous study (Santos et al., 2017).

2.13. Statistical analysis

In all of the datasets considered, the normality of the data was analyzed using the Anderson-Darling test, and homoscedasticity was analyzed with the variance equation test (or Levene's test). The results were subjected to statistical analysis using SAS statistical software – System for Windows 9.2. The means were compared using the Tukey test ($p < 0.05$).

3. Results

3.1. Dry mass production

Shoot dry mass production decreased with Ni levels equal to or higher than 0.1 μmol L^{-1} (Fig. 1A). The highest Ni levels (10 and 20 μmol L^{-1}) resulted in decreases of up to 41% relative to the mean dry mass production for plants grown with 0, 0.05, or 0.1 μmol L^{-1} Ni in the nutrient solution. It should be noted that in the present study, the nutrient solution was kept at pH 5 in order to intensify Ni toxicity. Root dry mass was more sensitive to Ni in the nutrient solution (Fig. 1B), decreasing with Ni levels higher than 0.05 μmol L^{-1}. However, the

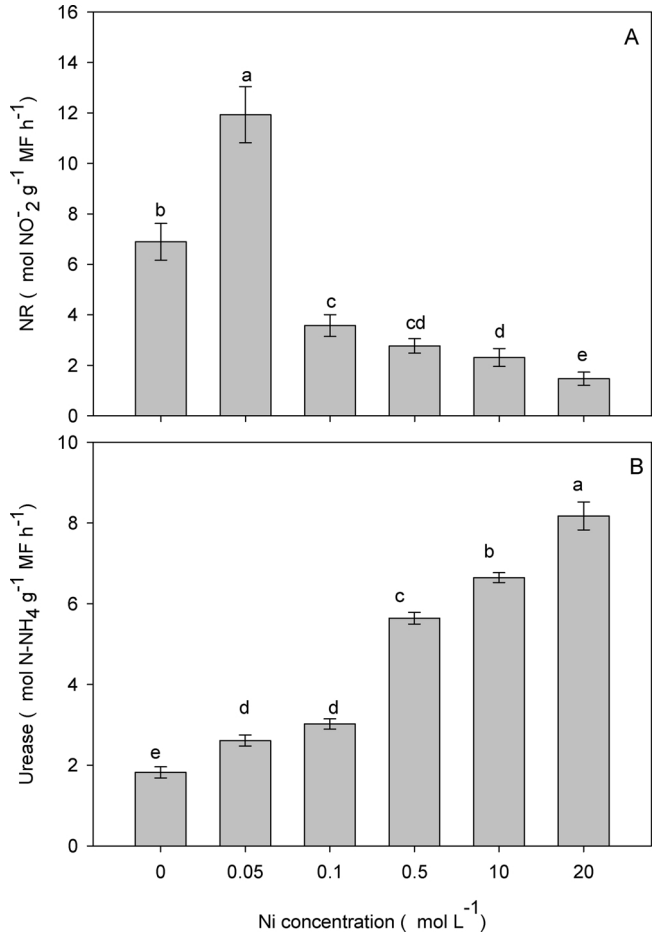

Fig. 3. Activity of nitrate reductase (A) and urease (B) in leaves of soybean plants grown at different Ni concentrations in the nutrient solution. Letters indicate statistically significant differences at $P \leq 0.05$. Error bars indicate the standard error (n = 4).

highest Ni levels (10 and 20 μmol L^{-1}) resulted in a decrease of approximately 37% relative to the control (0 μmol L^{-1}), similar to that observed for the shoot (Fig. 1A).

3.2. Gas exchange and nitrogen-assimilating enzymes

A, *Gs*, and *E* decreased with increasing Ni concentrations in the nutrient solution (Fig. 2A, B and C). The highest Ni concentration (20 μmol L^{-1}) decreased *A* by 98%, *Gs* by 92%, and *E* by 70% compared with plants grown at the lowest Ni concentration. It should be highlighted that decreases in *E* were only observed with 10 and 20 μmol L^{-1} Ni (Fig. 2C). In contrast to other gas exchange parameters, C_I was higher at the highest Ni concentrations (10 to 20 μmol L^{-1}) (Fig. 2D).

N metabolism enzymes responded differently to Ni concentrations in the nutrient solution. NR activity increased 84% with 0.05 μmol L^{-1} Ni relative to the control (Fig. 3A) but showed a pronounced decreased at the highest Ni concentrations. On the other hand, urease activity increased up to 300% with 20 μmol L^{-1} Ni relative to the control (Fig. 3B).

3.3. Antioxidant enzymes

Shoot soluble protein concentrations decreased 47% with increasing Ni levels (Fig. 4A). However, root soluble protein increased 27% with 0.05 μmol L^{-1} Ni and decreased 87% at the highest Ni concentrations in the nutrient solution (10 to 20 μmol L^{-1}) compared with the control.

Oxidative stress enzymes exhibited different behaviors. POD activity in shoots was highest at the highest Ni level (20 μmol L^{-1}), presenting a five-fold increase (Fig. 4C). However, POD activity in roots increased up to 10-fold with 10 μmol L^{-1} Ni (Fig. 4D).

SOD activity in shoots did not change significantly with 0.05 and 0.1 μmol L^{-1} Ni but was highest at the highest Ni concentration (20 μmol L^{-1}) (Fig. 4E). No significant differences in SOD activity in roots were observed between 0.05 μmol L^{-1} Ni and the control (Fig. 4F). SOD activity was highest for plants grown at the highest Ni levels (10–20 μmol L^{-1}), presenting a 10-fold increase relative to the control.

CAT activity behaved similarly in roots and shoots, increasing with up to 0.5 μmol L^{-1} Ni and then decreasing at increasing Ni levels (Fig. 4G and H).

3.4. Leaf and root morphology

Ni supplies higher than 0.05 μmol L^{-1} had a negative effect on the epidermal thickness of the leaf abaxial and adaxial surfaces (Figs. 5 A, B and 6), as well as on root phloem and xylem diameter (Figs. 5C, D and 7). This decrease in vascular tissues reached approximately 40% in roots and was more pronounced in the leaf adaxial and abaxial epidermis, reaching 50%.

The increase in Ni supply led to changes in leaf color due to Ni accumulation in leaves (Fig. 8). Increased leaf Ni concentrations promoted chlorosis and the predominance of brown color. It should be noted that leaf toxicity symptoms were more evident with 20 μmol L^{-1} Ni. Electron microscopy images of the abaxial (Fig. 9) and adaxial (Fig. 10) epidermis revealed detrimental effects proportional to the increase in leaf color. Increased Ni availability in the nutrient solution therefore increased cellular atrophy in the leaf epidermis. In addition, the leaf central vein region presented tissue disorganization with increasing Ni doses in the nutrient solution. Plants subjected to excess Ni displayed decreased root xylem and phloem diameters (Fig. 5C and D), indicating a detrimental effect of Ni toxicity (Fig. 7). Changes in leaf and root morphology due to toxicity caused by excess Ni were more pronounced in plants grown in 20 μmol L^{-1}.

3.5. Nutrient concentrations

No significant differences in shoot nutrient concentrations were observed between different Ni levels. However, significant differences were observed in root macro- and micronutrient concentrations (Fig. 11). The first effect of interionic interactions (competitive and non-competitive inhibition) on nutrient uptake is to change root nutrient uptake rates. Therefore, because of the exposure time in the present study (72 h), only effects on root nutrient uptake were observed. Phosphorus, Ca, and Mn concentrations decreased with increasing Ni concentrations in the nutrient solution (Fig. 11A, C and G). Changes in K concentrations were only observed at 10 and 20 μmol L^{-1} Ni (Fig. 11B), for which lower K concentrations were observed compared with the remaining treatments.

Different trends were observed for micronutrients. Boron and Zn concentrations increased with increasing Ni supply up to 1 and 0.5 μmol L^{-1}, respectively, and then decreased (Fig. 11D and H). Copper and Fe concentrations were higher for plants grown in 10 or 20 μmol L^{-1} Ni (Fig. 11E and F).

Mean Ni concentrations varied between 77.5 and 17,797.4 mg kg^{-1} in roots and between 2.3 and 16,774.5 mg kg^{-1} in shoots (Fig. 12). Soybean plants exhibited symptoms of Ni toxicity at Ni levels equal to or higher than 0.1 μmol L^{-1}, with a mean shoot Ni concentration of 28.9 mg kg^{-1}, and leaf water loss until complete drying (Fig. 8).

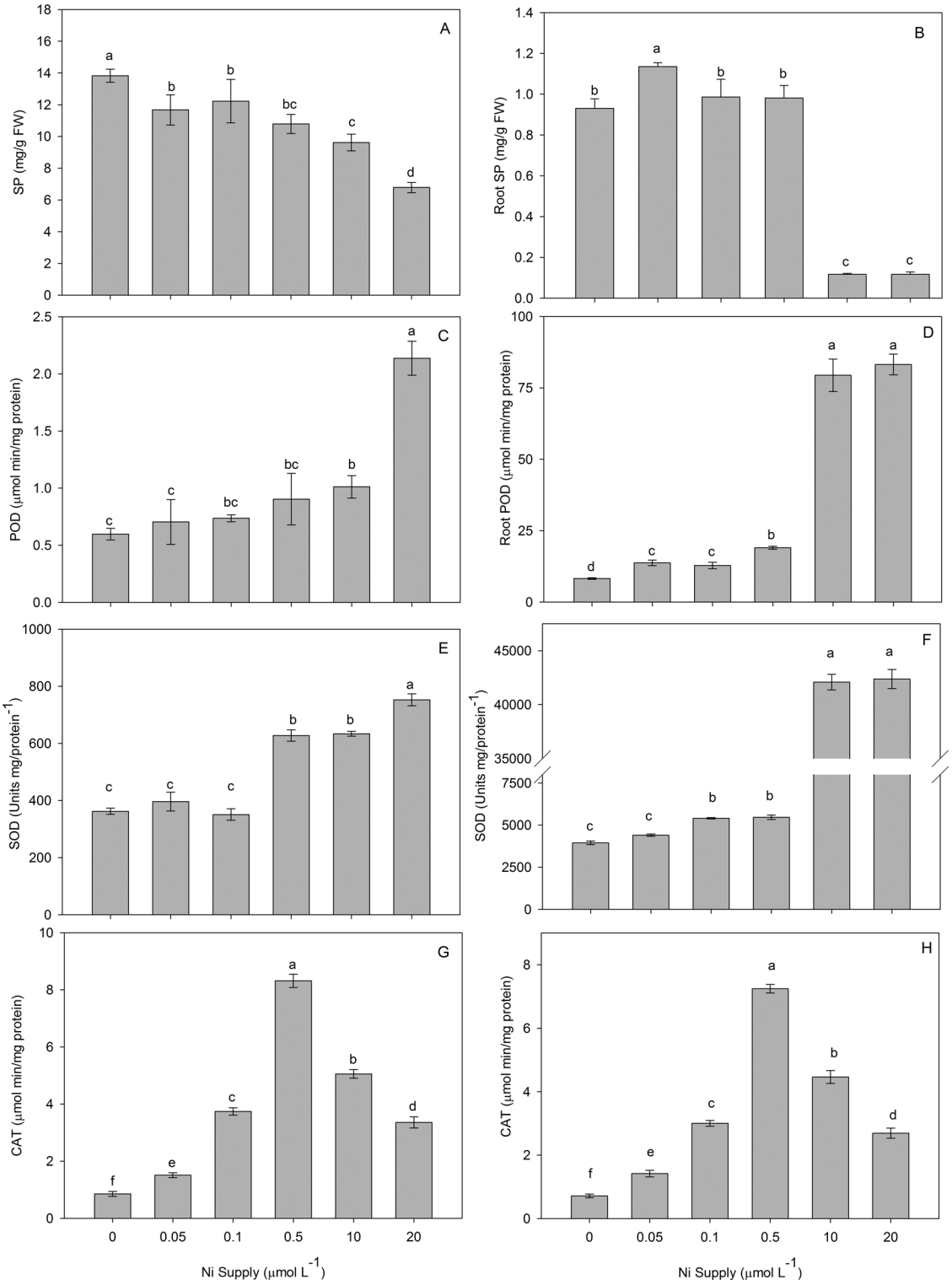

Fig. 4. Soluble protein concentration (A, B) and POD (C, D), SOD (E, F) and CAT (G, H) antioxidant activity in leaves and roots of soybean plants grown at different Ni concentrations in the nutrient solution. Letters indicate significant differences at $P \leq 0.05$. Error bars indicate the standard error (n = 4).

4. Discussion

4.1. Dry mass production, gas exchange and nitrogen-assimilating enzymes

Plant dry mass was affected by the Ni supply. Plant growth was not compromised with 0.05 μmol L^{-1} Ni in the nutrient solution, but higher Ni supplies led to excess Ni uptake, resulting in decreased photosynthetic activity (Fig. 2), visible toxicity symptoms, and subsequent tissue necrosis (Fig. 8). These effects were previously observed in corn (Drazkiewicz and Baszynki, 2010), *Populus nigra* (Velikova et al., 2011) and cauliflower (Shukla et al., 2015). It is noteworthy that the toxicity symptoms were found in plants grown at Ni supply in grown solution similar to the pore water free Ni in polluted soils (Nolan et al., 2009).

NR activity increased at 0.05 μmol L^{-1} Ni (Fig. 3A), whereas urease activity increased with increasing Ni concentrations in the nutrient solution (Fig. 3B). Soybean plants with adequate Ni concentrations

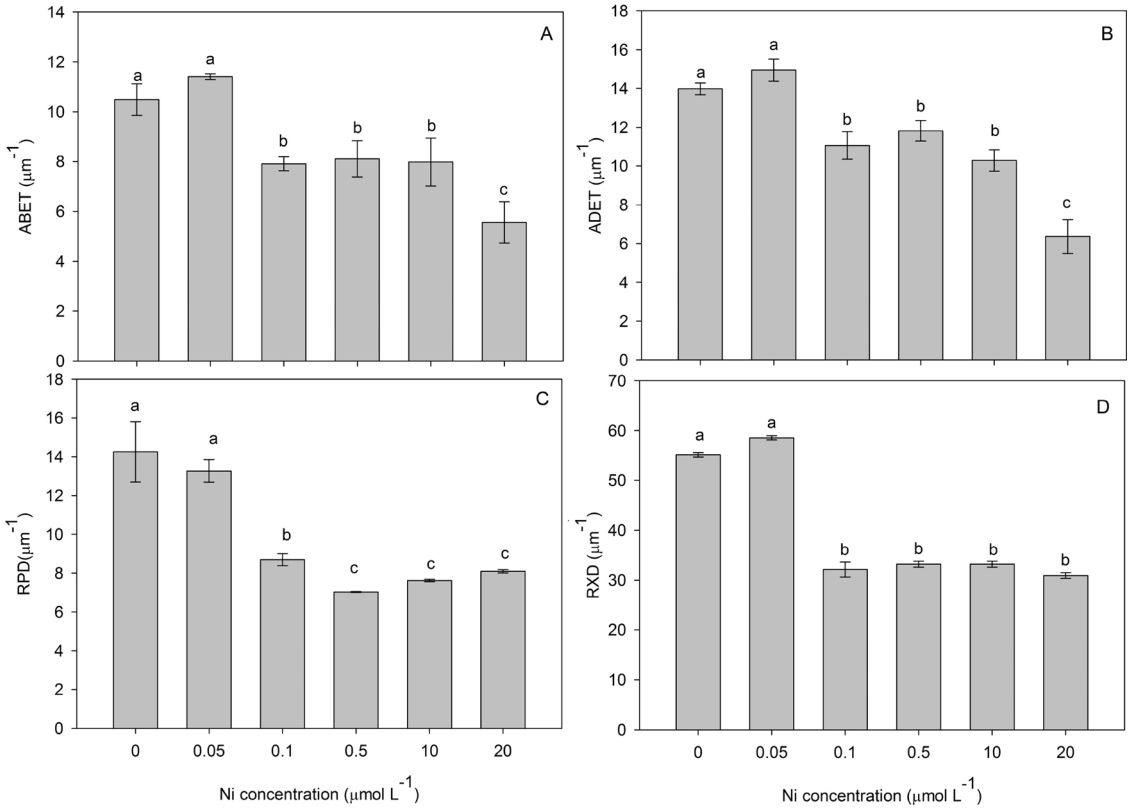

Fig. 5. Epidermal thickness of the lower or abaxial face (ABET) (A), epidermal thickness of the upper or adaxial face (ADET) (B), root phloem diameter (RPD) (C), and root xylem diameter (RXD) (D) of soybean plants in response to Ni concentrations in the nutrient solution. Letters indicate significant differences at $P \leq 0.05$. Error bars indicate the standard error (n = 4).

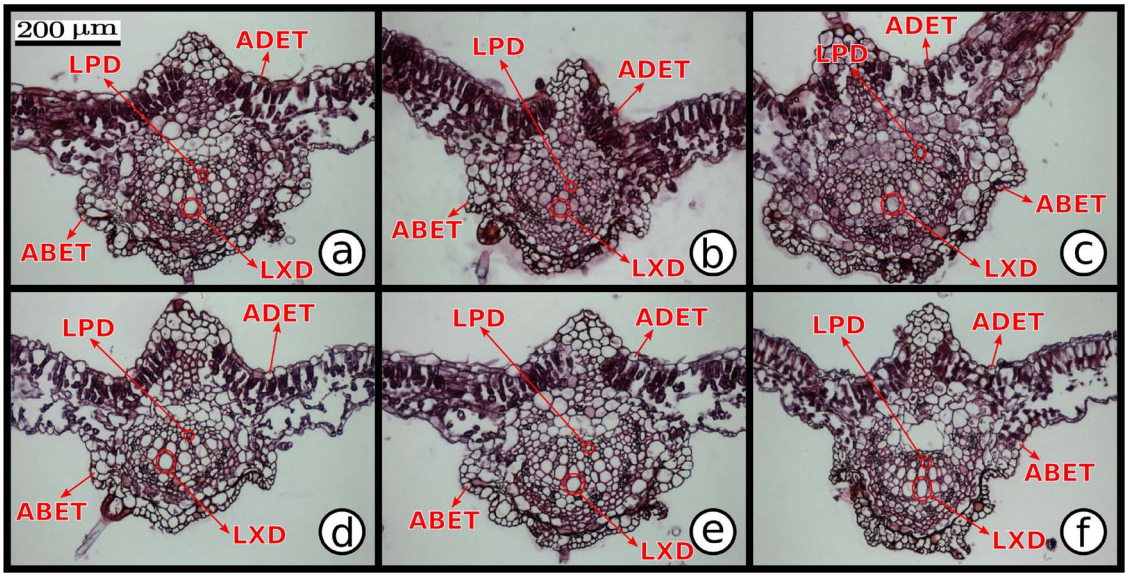

Fig. 6. Histological sections showing the xylem diameter (LXD), phloem diameter (LPD), and abaxial (ABET) and adaxial (ADET) surface thickness of soybean leaves. (A) Control, (B) 0.05 mmol L^{-1}, (C) 0.1 mmol L^{-1}, (D) 0.5 mmol L^{-1}, (E) 10 mmol L^{-1}, and (F) 20 mmol L^{-1}. Leaves were harvested after 7 days of exposure to Ni treatment.

present higher nitrate, urea, and protein- and free amino acid-N concentrations, leading to higher activity of N-assimilating enzymes (Kutman et al., 2013, 2014; Alibakhsh and Khoshgoftarmanesh, 2015). However, negative effects on NR activity were observed with increasing Ni levels. This difference may have been connected to NR degradation by ROS under Ni-toxicity conditions, as previously reported by Shukla et al. (2015). In addition, high Ni supply may decrease the uptake of Mo, which is an NR cofactor (Akpinar et al., 2015). These factors, together with the toxic effect of Ni on soybean, which affects plant growth and the photosynthetic apparatus (Figs. 1 and 2), negatively affected N metabolism, significantly affecting NR activity.

Plants exhibiting more evident symptoms of Ni toxicity (grown with 20 μmol L^{-1} Ni; Fig. 8D, E and F) presented higher urease activity (Fig. 3B). Under abiotic-stress conditions (e.g., Ni toxicity), arginine decarboxylase and ornithine decarboxylase activities increase. These enzymes are responsible for arginine degradation, releasing spermidine

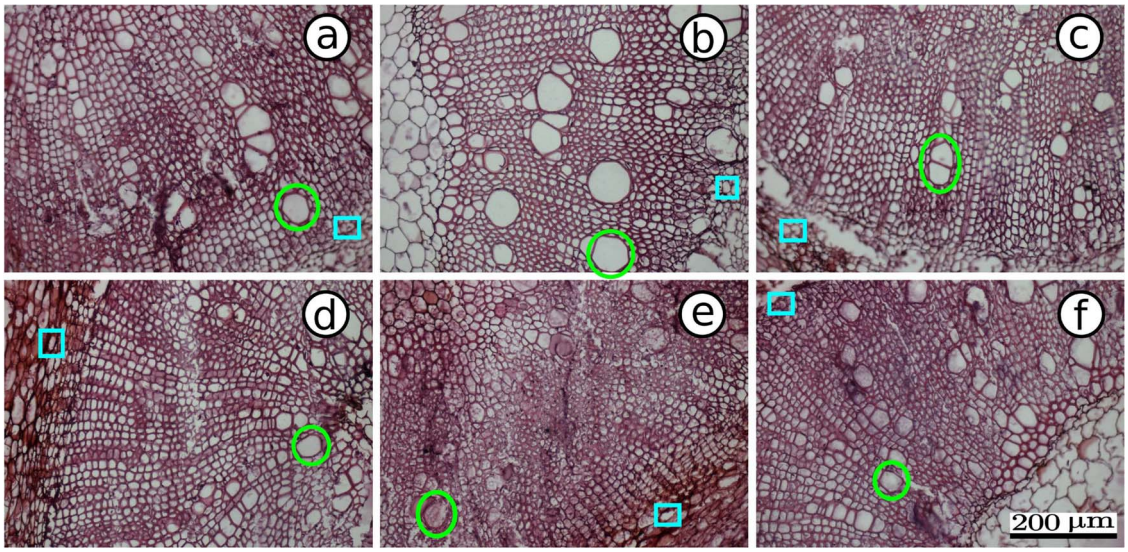

Fig. 7. Histological sections showing the root xylem diameter (green circle) and root phloem diameter (blue square) of soybean plants. (A) Control, (B) 0.05 mmol L^{-1}, (C) 0.1 mmol L^{-1}, (D) 0.5 mmol L^{-1}, (E) 10 mmol L^{-1}, and (F) 20 mmol L^{-1}. The leaves were harvested after 7 days of exposure to Ni treatment. (For interpretation of the references to colour in this figure legend, the reader is referred to the web version of this article.)

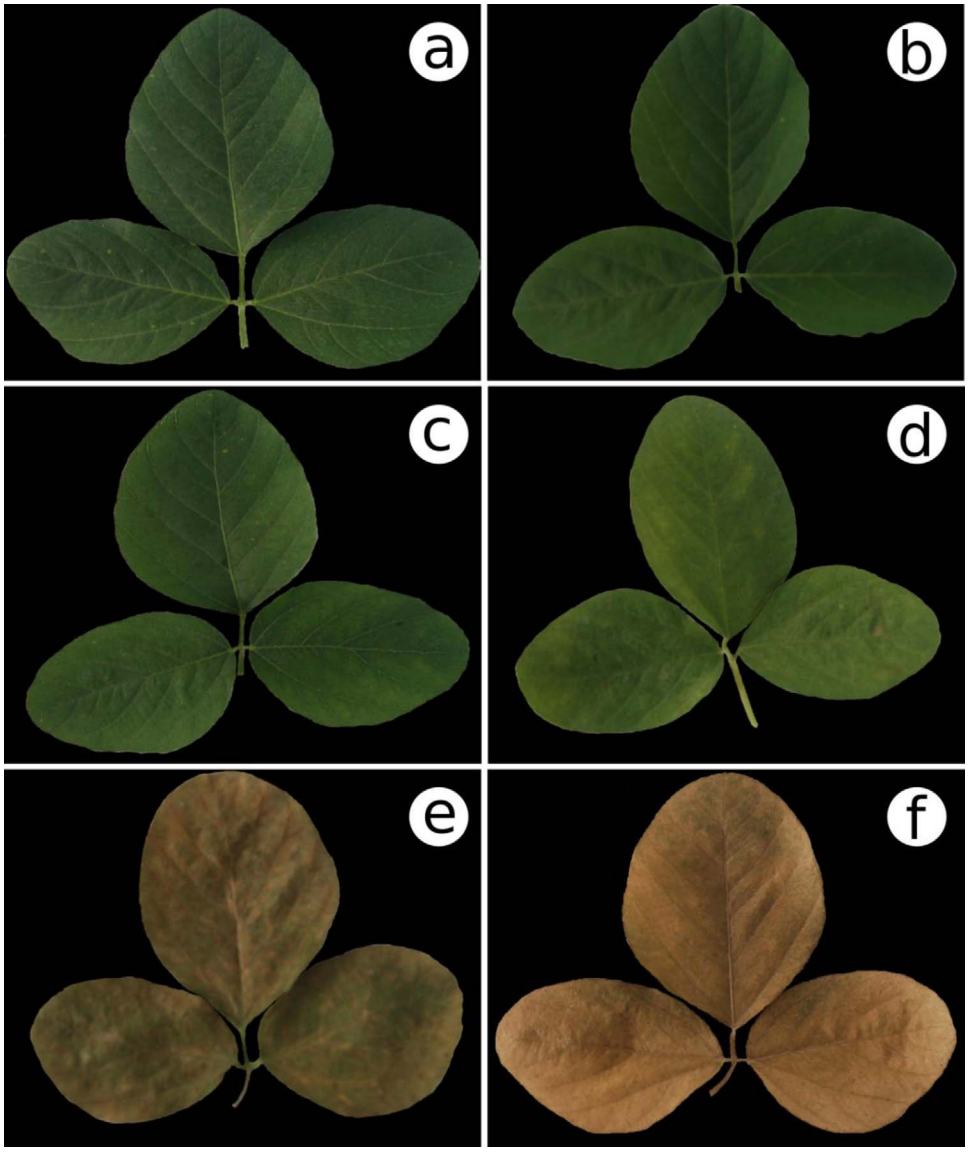

Fig. 8. Soybean leaves showing Ni toxicity symptoms. (A) Control, (B) 0.05 mmol L^{-1}, (C) 0.1 mmol L^{-1}, (D) 0.5 mmol L^{-1}, (E) 10 mmol L^{-1}, and (F) 20 mmol L^{-1}. Leaves were harvested after 7 days of exposure to Ni treatment.

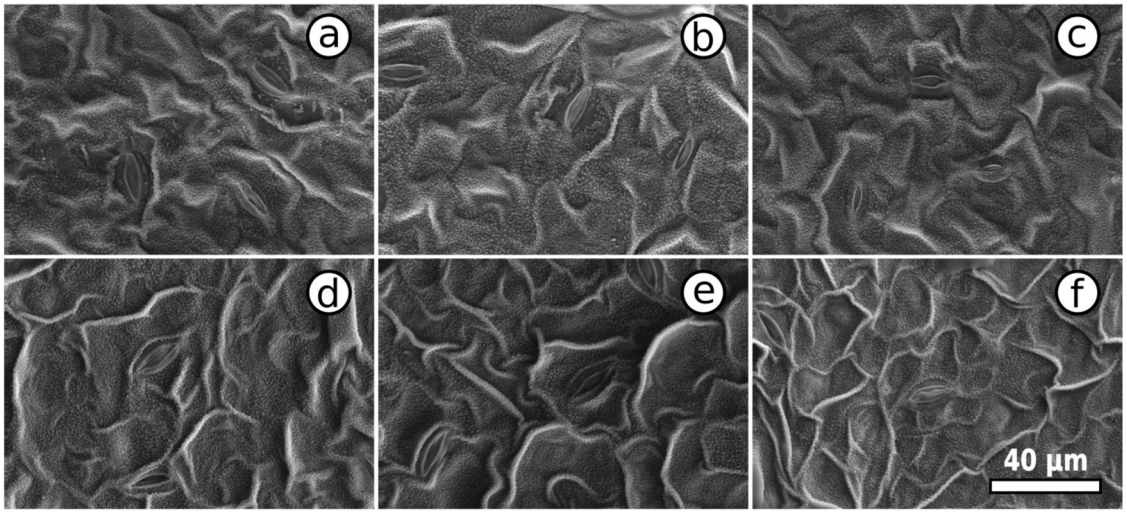

Fig. 9. Scanning electron micrographs showing the abaxial part of soybean leaves under Ni treatment collected after 7 days of exposure. (A) Control, (B) 0.05 mmol L^{-1}, (C) 0.1 mmol L^{-1}, (D) 0.5 mmol L^{-1}, (E) 10 mmol L^{-1}, and (F) 20 mmol L^{-1}. Leaves were harvested after 7 days of exposure to Ni treatment.

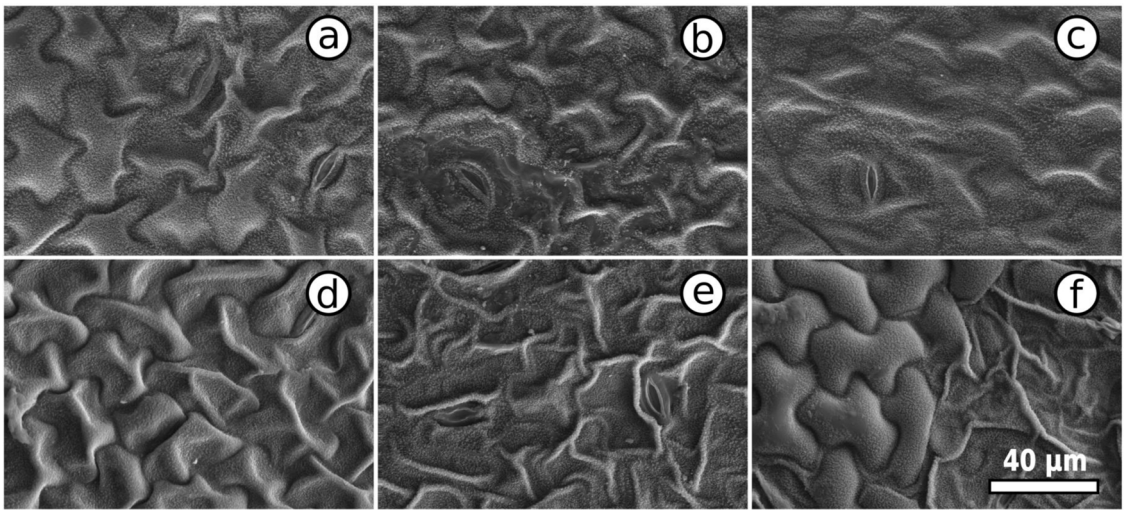

Fig. 10. Scanning electron micrographs showing the adaxial part of soybean leaves under Ni treatment collected after 7 days of exposure. (A) Control, (B) 0.05 mmol L^{-1}, (C) 0.1 mmol L^{-1}, (D) 0.5 mmol L^{-1}, (E) 10 mmol L^{-1}, and (F) 20 mmol L^{-1}. Leaves were harvested after 7 days of exposure to Ni treatment.

and spermine inside mitochondria and urea into the cytosol (Talaat and Shawky, 2016). Urea release into the cytosol increases urease activity (Polacco et al., 2013), similar to that observed in the present study (Fig. 3B). Thus, the observed increase in urease activity was likely a response to arginine degradation and the consequent increase in the cytosolic urea concentration. In addition, the higher Ni uptake in plants grown in 20 µmol L^{-1} Ni (Fig. 12) also stimulated urease activity. A correlation between leaf Ni concentrations and urease activity has been previously reported for soybean (Macedo et al., 2016).

The decrease in *A*, *Gs* and *E* and increase in C_I (Fig. 2) indicated a toxic effect on the photosynthetic apparatus of soybean plants. Metal toxicity increases the concentration of ROS, which decrease the quantum yield and Hill reaction activity and degrade chlorophyll (Pietrini et al., 2015; Shukla et al., 2015; Sirhindi et al., 2016). The lower *A* combined with higher C_I − partly due to lower *Gs*, i.e., closed stomata − indicate that Ni toxicity, in addition to the common metal toxic effects on photosynthesis, also decreases the C fixation capacity of soybean plants. The observed changes in the organization and conformation of root xylem and phloem (Fig. 5C and D) also resulted in lower *E*. Changes to the root vessels lead to decreased turgor in shoot tissues, cause stomatal closure on the adaxial and abaxial leaf surface, and promote disorganization of leaf tissues (Pietrini et al., 2015; Armendariz et al., 2016), as observed in the present study (Figs. 5A, B and 6).

4.2. Antioxidant enzymes

Decreasing plant soluble protein concentrations may have a direct effect on Ni toxicity. High Ni concentrations in leaf tissues (Fig. 12) induce the accumulation of Ni in the cationic form (Ni^{2+}), which can change the chromatin protein profile and result in genotoxic effects, resulting in decreased soluble protein content (Erturk et al., 2016). In addition, Ni^{2+} can also affect cytokinin methylation, causing DNA hypo- or hypermethylation. Under conditions of hypomethylation, chromosomes are more susceptible to breaks, whereas hypermethylation causes chromosome instability, with detrimental effects to cells (Kovalchuk et al., 2001), decreasing protein synthesis and increasing free amino acid content (El Shintinawy and El Ansary, 2000).

CAT activity increased only at 0.5 µmol L^{-1} Ni (Fig. 4G and H), whereas the same was not observed for SOD and POD (Fig. 4). SOD and POD activity increased with increasing Ni concentrations in the nutrient solution. The decrease in CAT activity can be attributed to excess production of ROS, which have their ligand in an inactivated heme group (Willekens et al., 1997). Cakmak and Horst (1991) suggested that

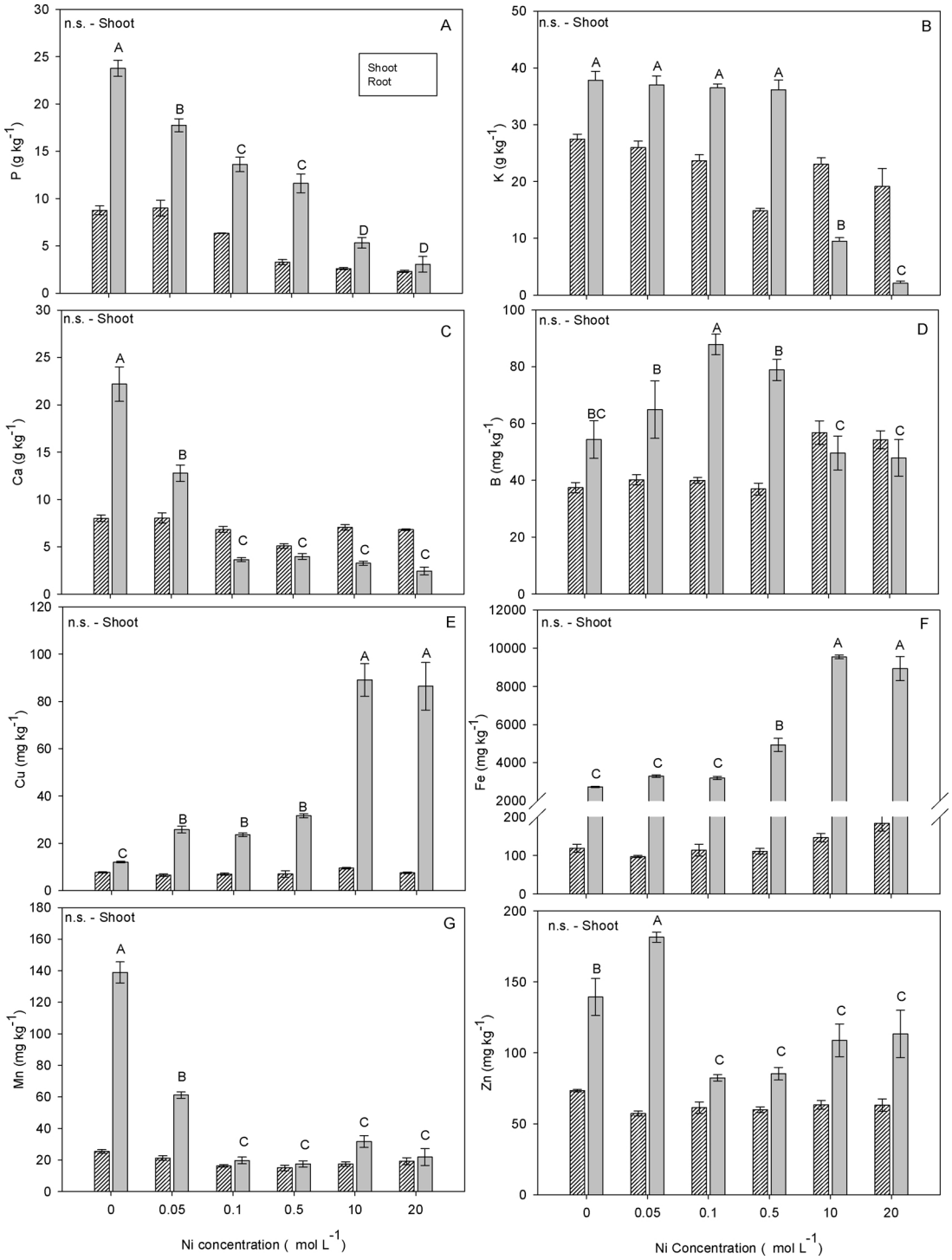

Fig. 11. Phosphorus (A), K (B), Ca (C), B (D), Cu (E), Fe (F), Mn (G), and Zn (H) concentrations in the shoots and roots of soybean plants grown at different Ni concentrations in the nutrient solution. Error bars indicate the standard error (n = 4). Different lowercase letters indicate significant differences in shoots, and different uppercase letters indicate significant differences in roots, according to the Tukey test ($P < 0.05$). ns: non-significant.

decreased CAT activity and increased POD activity in plants under stress conditions indicate that the generated H_2O_2 is mostly consumed by oxidative processes, such as lipid peroxidation.

SOD and POD activity in roots increased significantly at toxic Ni levels (Fig. 4D and F), similar to observations by Gajewska and Skłodowska (2005). Ni uptake by roots causes increased NADPH oxidase activity, peaking only 12 h after Ni supplementation (Hao et al., 2006). In addition, excess Ni results in increased O_2^- and H_2O_2 concentrations, the latter originating from O_2^- dismutation by SOD (Hao et al., 2006).

The increase in antioxidant enzyme activity at increasing Ni concentrations in the nutrient solution was less pronounced in shoots than in roots, probably due to decreased long-distance transportation and Ni accumulation in shoots at the time of evaluation. In wheat, after a 48-h exposure to Ni in the nutrient solution, only 35% of the total Ni taken by plants was translocated to the shoots (Dalir and Khoshgoftarmanesh, 2014). However, the increasing Ni supplies were sufficient to induce an increase in root antioxidant enzyme activity of up to fourfold relative to

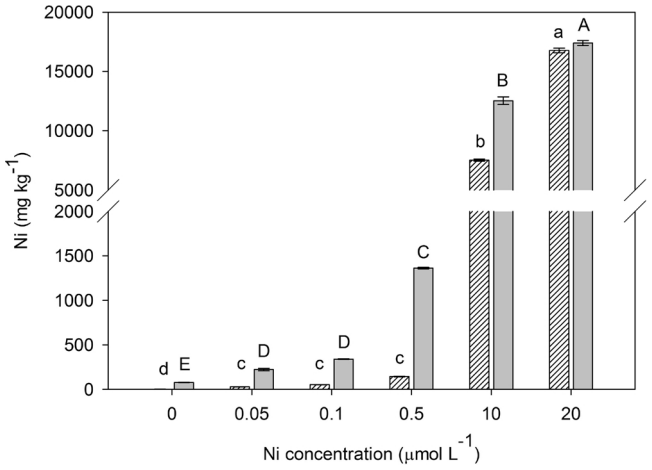

Fig. 12. Ni concentrations in the shoots and roots of soybean plants grown at different Ni concentrations in the nutrient solution. Error bars indicate the standard error (n = 4). Different lowercase letters indicate significant differences in shoots, and different uppercase letters indicate significant differences in roots, according to the Tukey test ($P < 0.05$). ns: non-significant.

control plants (Fig. 4C, D and G).

CAT activity presented very similar behavior in roots and shoots (Fig. 4G and H) but differed slightly from the behavior of the remaining oxidative stress enzymes. This difference was due to the proteolytic degradation of CAT in peroxisomes when leaves undergo senescence (Distefano et al., 1999), leading to CAT inactivation with increasing heavy-metal stress. Decreased CAT activity was reported to be compensated by increased POD activity in *Brassica napus* (Nouairi et al., 2009), which was also observed in the present study.

4.3. Ni toxicity symptoms and leaf and root ultrastructural changes

The detrimental effect of high Ni supplies on plant metabolism directly affected sap and photoassimilate transport by reducing the root phloem and xylem diameter (Fig. 5C and D), showing that Ni supplies above 0.05 µmol L^{-1} had a negative effect on leaf tissue development (Figs. 6 and 8).

The observed brown color on soybean leaves (Fig. 8C and D) was induced by the presence of Ni inside leaf cells. High leaf Ni concentrations induced the production of plastoglobules, which act as a plant defense mechanism (Pookothai and Vijayavathi, 2012). Increases in the number and size of plastoglobules in chloroplasts negatively affect the synthesis of lipid bodies, which help protect the photosynthetic apparatus against free radicals (Moraes et al., 2014). These Ni toxicity symptoms were also observed in the leaves of cabbage (Molas, 1997), wheat (Seregin and Kozhevnikova, 2006), and cauliflower (Shukla et al., 2015). These authors also observed decreased mesophyll thickness and epidermal cell width, as well as smaller vascular bundles. It should be noted that the decrease in leaf epidermal thickness observed in the present study directly affects resistance to mechanical, chemical and biological damage. This finding is in agreement with Seregin and Kozhevnikova (2006), who reported detrimental effects of Ni on internal leaf morphology.

4.4. Macro- and micronutrient concentrations

Ni uptake is a multiphasic process (more than one isotherm is needed to describe uptake velocity), and Ni is transported via the xylem as complexes or organic anion chelates. Under toxicity conditions, Ni uptake is compromised, and high leaf Ni concentrations antagonize similar ions. In the present study, P, K, Ca, Mn, and Zn uptake was observed to decrease (Fig. 11). This decrease was mainly due to the toxic effect of Ni on plant growth. The uptake of these nutrients was therefore compromised in plants grown in the highest Ni levels, resulting in lower P, K, Ca, Mn and Zn concentrations in roots. However, root Cu and Fe concentration was observed to increase.

The interaction between Ni and Cu is antagonistic, and competition between them has been observed in soybean (Cataldo et al., 1978) and barley (Korner et al., 1987). On the other hand, Ni toxicity in the field is often associated with Cu toxicity, indicating a synergy between the two, although this effect is not well understood (Küpper and Andresen, 2016). The same can be said about the interaction between Ni and Fe since the presence of Ni has been reported to decrease Fe uptake. Nishida et al. (2015) studied Ni uptake by Fe transporters and observed that Ni not only uses Fe transporters but also induces plants to produce more Fe transporters, which may have resulted in higher Fe uptake by roots. In the present study, exudation of organic acids by roots may have favored Ni and Fe uptake by roots.

5. Conclusions

Soybean plants exhibited symptoms of Ni toxicity starting at 0.1 µmol L^{-1} Ni, corresponding to a shoot Ni concentration of 28.9 mg kg^{-1}, presenting decreased carbon dioxide assimilation and shoot and root dry mass.

The activity of antioxidant enzymes – CAT, POD and SOD – increased in roots and shoots with increasing Ni uptake. Root xylem and phloem diameter, as well as leaf adaxial and abaxial epidermal thickness, decreased starting at 0.1 µmol L^{-1} Ni. These results contribute to our understanding of several basic mechanisms of Ni toxicity in soybean, which remains poorly understood.

Acknowledgements

This work was financially supported by a grant from the National Council for Scientific and Technological Development (Grant 448783/2014-2). The authors would like to thank the CAPES Foundation for studentship (JPQB) and (JMKS) granted.

References

Ahmad, M.S.A., Hussain, M., Saddiq, R., Alvi, A.K., 2007. Mung bean: a nickel indicator: accumulator or excluder. Bull. Environ. Contam. Toxicol. 78, 319–324.
Ahmad, P., Sarwat, M., Bhat, N.A., Wani, M.R., Kazi, A.G., Tran, L.S.P., 2015. Alleviation of cadmium toxicity in Brassica juncea L. (Czern. & Coss.) by calcium application involves various physiological and biochemical strategies. PLoS One 10, e0114571.
Ahmad, P., 2013. Oxidative Damage to Plants, Antioxidant Networks and Signaling. Academic Press, Cambridge, MA.
Akpinar, A., Arslan, H., Güleryüz, G., Kırmızı, S., Erdemİr, Ü.S., Güçer, Ş., 2015. Ni-induced changes in nitrate assimilation and antioxidant metabolism of verbascum olympicum boiss.: could the plant be useful for phytoremediation or/and restoration purposes? Int. J. Phytorem. 17, 546–555.
Alibakhsh, M., Khoshgoftarmanesh, A.H., 2015. Effects of nickel nutrition in the mineral form and complexed with histidine in the nitrogen metabolism of onion bulb. Plant Growth Regul. 75, 733–740.
Allain, C.C., Poon, L.S., Chan, C.S.G., Richmond, W., Fu, P.C., 1974. Enzymatic determination of total serum cholesterol. Clin. Chem. 120, 470–475.
Armendariz, A.L., Talano, M.A., Villasuso, A.L., Travaglia, C., Racagni, G.E., Reinoso, H., Agostini, E., 2016. Arsenic stress induces changes in lipid signalling and evokes the stomata closure in soybean. Plant Physiol. Biochem. 103, 45–52.
Azevedo, R.A., Alas, R.M., Smith, R.J., Lea, P.J., 1998. Response of antioxidant enzymes to transfer from elevated carbon dioxide to air and ozone fumigation, in the leaves and roots of wild-type and a catalase-deficient mutant of barley. Physiol. Plant. 104, 280–292.
Bishnoi, N.R., Sheoran, I.S., Singh, R., 1993. Influence of cadmium and nickel on photosynthesis and water relations in wheat leaves of different insertion level. Photosynthetica 28, 473–479.
Bradford, M.M., 1976. A rapid and sensitive method for the quantitation of microgram quantities of protein utilizing principle of protein-dye-binding. Anal. Biochem. 72, 248–254.
Cakmak, I., Horst, W.J., 1991. Effect of aluminium on lipid peroxidation, superoxide dismutase, catalase, and peroxidase activities in root tips of soybean (Glycine max). Physiol. Plant. 83, 463–468.
Carlquist, S.J., 1975. Ecological strategies of xylem evolution. University of California Press, Berkley CA.
Cataldo, D.A., Garland, T.R., Wildung, R.E., 1978. Nickel in plants. I: Uptake kinetics using intact soybean seedlings. Plant Physiol. 62, 5636–5665.

Dalir, N., Khoshgoftarmanesh, A.H., 2014. Symplastic and apoplastic uptake and root to shoot translocation of nickel in wheat as affected by exogenous amino acids. J. Plant Physiol. 171, 531–536.
Distefano, S., Palma, J.M., McCarthy, I., del Rio, L.A., 1999. Proteolytic cleavage of plant proteins by peroxisomal endoproteases from senescent pea leaves. Planta 209 (3), 308–313.
Dixon, N.E., Gazzola, C., Brakeley, R.L., Zerne, B., 1975. Jack-bean urease (EC 3.5.1.5.3). metalloenzyme. a simple biological role for nickel. J. Am. Chem. Soc. 97 (14), 4131–4133.
Drazkiewicz, M., Baszynki, T., 2010. Interference of nickel with the photosynthetic apparatus of Zea mays. Ecotoxicol. Environ. Saf. 73, 982–986.
El Shintinawy, F., El Ansary, A., 2000. Differential effect of Cd2+ and Ni2+ on amino acid metabolism in soybean seedlings. Biol. Plant. 43 (1), 79–84.
Erturk, F.A., Ay, H., Nardemir, G., 2016. Molecular determination of genotoxic effects of cobalt and nickel on maize (Zea mays L.) by RAPD and protein analyses. Toxicol. Ind. Health 29, 662–671.
Fabiano, C.C., Tezotto, T., Favarin, J.L., Polacco, J.C., Mazzafera, P., 2015. Essentiality of nickel in plants: a role in plant stresses. Front. Plant Sci. 6, 754. http://dx.doi.org/10.3389/fpls.2015.00754.
Gajewska, E., Skłodowska, M., 2005. Antioxidative responses and proline level in leaves and roots of pea plants subjected to nickel stress. Acta Physiol. Plant. 27 (3), 329–340.
Gajewska, E., Sklodowska, M., Slaba, M., Mazur, J., 2006. Effect of nickel on antioxidative enzyme activities: proline and chlorophyll contents in wheat shoots. Biol. Plant. 50, 653–659.
Giannopolitis, C.N., Ries, S.K., 1977. Superoxide dismutases: I. Occurrence in higher plants. Plant Physiol. 59 (2), 309–314.
Granick, S., 1951. Biosynthesis of chlorophyll and related pigments. Annu. Rev. Plant Physiol. 2, 115–144.
Gustafsson, J.P., 2011. Visual MINTEQ Ver. 3.0. KTH. Department of Land and Water Resources Engineering. http://www2.lwr.kth.se/English/OurSoftware/vminteq/.
Hao, F., Wang, X., Chen, J., 2006. Involvement of plasma-membrane NADPH oxidase in nickel-induced oxidative stress in roots of wheat seedlings. Plant Sci. 170 (1), 151–158.
Hewitt, E.J., 1953. Metal interrelationship in plant nutrition. J. Exp. Bot. 4 (1), 59–64.
Hoagland, D.R., Arnon, D.I., 1950. The Water-Culture Method for Growing Plants Without Soil. California Agricultural Experiment Station Circular 347. College of Agriculture, University of California, Berkeley.
Hogan, M.E., Swift, I.E., Done, J., 1983. Urease assay and ammonia release from leaf tissues. Phytochemistry 22, 663–667.
Küpper, H., Andresen, E., 2016. Mechanisms of metal toxicity in plants. Metallomics 8, 269–285.
Küpper, H., Kroneck, P.M.H., 2007. Nickel in the environment and its role in the metabolism of plants and cyanobacteria. In: In: Sigel, A., Sigel, H., Sigel, R.K.O. (Eds.), Nickel and Its Surprising Impact in Nature, vol. 2 Wiley J. Ltd., West Sussex (ch. 5, pp. 31).
Kabata-Pendias, A., Pendias, H., 2011. Trace Elements in Soil and Plants, vol. 4 CRC Press (548 p).
Kazemi, N., Khavari-Nejad, R.A., Fahimi, H., Saadatmand, S., Nejad-Sattari, T., 2010. Effects of exogenous salicylic acid and nitric oxide on lipid peroxidation and antioxidant enzyme activities in leaves of Brassica napus L. under nickel stress. Sci. Hortic.-Amsterdam 126 (3), 402–407.
Korner, L.E., Moller, L., Jensén, M.P., 1987. Effects of Ca2+ and other divalent cations on uptake of Ni2+ by excised barley roots. Physiol. Plant. 71, 49–54.
Kovalchuk, O., Titov, V., Hohn, B., Kovalchuk, I., 2001. A sensitive transgenic plant system to detect toxic inorganic compounds in the environment. Nat. Biotechnol. 19, 568–572.
Kutman, B.Y., Kutman, U.B., Cakmak, I., 2013. Nickel-enriched seed and externally supplied nickel improve growth and alleviate foliar urea damage in soybean. Plant Soil 363, 61–75.
Kutman, B.Y., Kutman, U.B., Cakmak, I., 2014. Effects of seed nickel reserves or externally supplied nickel on the growth, nitrogen metabolites and nitrogen use efficiency of urea- or nitrate-fed soybean. Plant Soil 376, 261–276.
Lavres Junior, J., Malavolta, E., Nogueira, N.L., Moraes, M.F., Reis, A.R., Rossi, M.L., Cabral, C.P., 2009. Changes in anatomy and root cell ultrastructure of soybean genotypes under manganese stress. R. Bras. Ciê. Solo 33, 395–403.
Lavres Junior, J., Reis, A.R., Rossi, M.L., Cabral, C.P., Nogueira, N.L., Malavolta, E., 2010. Changes in the ultrastructure of three soybean cultivars in response to manganese supply in solution culture. Sci. Agric. 67, 287–294.
Lavres, J., Castro, F.G., de Sousa Câmara, G.M., 2016. Soybean seed treatment with nickel improves biological fixation and urease activity. Front. Environ. Sci. 4, 1–11.
Macedo, F.G., Bresolin, J.D., Santos, E.F., Furlan, F., Silva, W.T., Polacco, J.C., Lavres, J., 2016. Nickel availability in soil as influenced by liming and its role in soybean nitrogen metabolism. Front. Plant Sci. 7, 1358. http://dx.doi.org/10.3389/fpls.2016.01358.
McCullough, H., 1967. The determination of ammonia in whole blood by a direct colorimetric method. Clín. Chim. Acta 17, 297–304.
Miller, R.O., 1998. Nitric-perchloric acid wet digestion in an open vessel. In: Karla, Y.P. (Ed.), Handbook of Reference Methods for Plant Analysis. CRC Press, Boca Raton, FL (pp. 57e61).
Mishra, D., Kar, M., 1974. Nickel in plant growth and metabolism. Bot. Rev. 40, 395–452.
Mohanty, N., Vaas, I., Demeter, S., 1989. Impairment of photosystem 2 activity at the level of secondary quinone electron acceptor in chloroplasts treated with cobalt nickel and zinc ions. Physiol. Plant. 76, 386–390.
Molas, J., 1997. Changes in morphological and anatomical structure of cabbage (Brassica oleracea L.) outer leaves and in ultrastructure of their chloroplasts caused by an in vitro excess of nickel. Photosynthetica 34, 513–522.
Moraes, C.L., Marini, P., Fernando, J.A., Moraes, D.M., Castro, L.A.S., Lopes, N.F., 2014. Physiological and ultra-structural changes in tomato seedlings induced by lead. Iheringia Serie Bot. 69, 313–322 (In Portuguese).
Nishida, S., Kato, A., Tsuzuki, C., Yoshida, J., Mizuno, T., 2015. Induction of nickel accumulation in response to zinc deficiency in Arabidopsis thaliana. Intern. J. Mol. Sci. 16, 9420–9430.
Nolan, A.L., Ma, Y., Lombi, E., McLaughlin, M.J., 2009. Speciation and isotopic exchangeability of nickel in soil solution. J. Environ. Qual. 38 (2), 485–492.
Nouairi, I., Ben Ammar, W., Ben Youssef, N., Ben Miled, D.D., Ghorbal, M.H., Zarrouk, M., 2009. Antioxidant defense system in leaves of Indian mustard (Brassica juncea) and rape (Brassica napus) under cadmium stress. Acta Physiol. Plant. 31, 237–247.
Pandolfini, T., Gabbrielli, R., Comparini, C., 1992. Nickel toxicity and peroxidase activity in seedlings of Triticum aestivum L. Plant. Cell Environ. 15, 719–725.
Pietrini, F., Iori, V., Cheremisina, A., Shevyakova, N.I., Radyukina, N., Kuznetsov, V.V., Zacchini, M., 2015. Evaluation of nickel tolerance in Amaranthus paniculatus L. plants by measuring photosynthesis oxidative status, antioxidative response and metal-binding molecule content. Environ. Sci. Pollut. Res. Int. 22, 482–494.
Polacco, J.C., Mazzafera, P., Tezotto, T., 2013. Opinion-Nickel and urease in plants: still many knowledge gaps. Plant Sci. 199, 79–90.
Pookothai, M., Vijayavathi, B.S., 2012. Nickel as an essential element and a toxicant. Intern. J. Environ. Sci. 1, 285–288.
Reis, A.R., Favarin, J.L., Gallo, L.A., Malavolta, E., Moraes, M.F., Lavres Junior, J., 2009. Nitrate reductase and glutamine synthetase activity in coffee leaves during fruit development. Rev. Bras. Ciê. Solo 33, 315–324.
Reis, A.R., Favarin, J.L., Gratão, P.L., Capaldi, F.R., Azevedo, R.A., 2015. Antioxidant metabolism in coffee (Coffea arabica L.) plants in response to nitrogen supply. Theor. Exp. Plant Physiol. 1, 1–11.
Ruter, J.M., 2005. Effect of nickel applications for the control of mouse ear disorder on river birch. J. Environ. Hort. 23, 17–20.
Santos, E.F., Santini, J.M.K., Paixão, A.P., Furlani Júnior, E., Lavres, J., Campos, M., Reis, A.R., 2017. Physiological highlights of manganese toxicity symptoms in soybean plants: mn toxicity responses. Plant Physiol. Biochem. 113, 6–19.
Schickler, H., Caspi, H., 1999. Response of antioxidative enzymes to nickel and cadmium stress in hyperaccumulator plants of the genus Alyssum. Physiol. Plant. 105, 39–44.
Seregin, I.V., Ivanov, V.B., 2001. Physiological aspects of cadmium and lead toxic effects on higher plants. Russ. J. Plant Physiol. 48 (4), 523–544.
Seregin, I.V., Kozhevnikova, A.D., 2006. Physiological role of nickel and its toxic effects on higher plants. Russ. J. Plant Physiol. 53, 257–277.
Sheoran, I.S., Singal, H.R., Singh, R., 1990. Effect of cadmium and nickel on photosynthesis and the enzymes of the photosynthetic carbon reduction cycle in pigeonpea (Cajanus cajan L.). Photosynth. Res. 23, 345–351.
Shukla, R., Sharma, Y.K., Gopal, R., 2015. Evaluation of toxicity level of nickel on growth photosynthetic efficiency, antioxidative enzyme, and its accumulation in cauliflower. Commun. Soil Sci. Plant Anal. 46, 2866–2876.
Sirhindi, G., Mir, M.A., Abd-Allah, E.F., Ahmad, P., Gucel, S., 2016. Jasmonic acid modulates the physio-biochemical attributes, antioxidant enzyme activity, and gene expression in Glycine max under nickel toxicity. Front. Plant Sci. 7, 1–12.
Sreekanth, T., Nagajyothi, P., Lee, K., Prasad, T., 2013. Occurrence: physiological responses and toxicity of nickel in plants. Int. J. Environ. Sci. Technol. 10, 1129–1140.
Talaat, N.B., Shawky, B.T., 2016. Dual application of 24-epibrassinolide and spermine confers drought stress tolerance in maize (Zea mays L.) by modulating polyamine and protein metabolism. J. Plant Growth Regul. 35, 518–533.
Tripathy, B.C., Bhatia, B., Mohanty, P., 1983. Cobalt ions inhibit electron transport activity of photosystem II without affecting photosystem I. Biochem. Biophys. Acta 722, 88–93.
Uren, N.C., 1992. Forms reactions, and availability of nickel in soils. Adv. Agron. 48, 141–203.
Velikova, V., Tsonev, T., Loreto, F., Centritto, M., 2011. Changes in photosynthesis mesophyll conductance to CO2, and isoprenoid emissions in Populus nigra plants exposed to excess nickel. Environ. Pollut. 159, 1058–1066.
White, P.J., 2012. Long-distance transport in the xylem and phloem. In: Marscher, P. (Ed.), Marschner's Mineral Nutrition of Higher Plants, 3rd ed. Academic Press, London, pp. 49–70.
Willekens, H., Chamnongpol, S., Davey, M., Schaudner, M., Langebartels, C., Van Montagu, M., Inzé, D., Van Camp, W., 1997. Catalase is a sink for H2O2 and is indispensable for stress defence in C3 plants. EMBO J. 16, 4806–4816.
Wood, B.W., Reilly, C.C., Nyczepir, A.P., 2006. Field deficiency of nickel in trees: symptoms and causes. Acta Hortic. 721, 83–97.